Available online at www.sciencedirect.com

SciVerse ScienceDirect

journal homepage: www.elsevier.com/locate/ijrefrig

Performance of a tube-in-tube CO_2 gas cooler

Pei-Yu Yu [a,c], Kai-Hsiang Lin [b], Wei-Keng Lin [c], Chi-Chuan Wang [b,*]

[a] Green Energy Research Laboratories, Industrial Technology Research Institute, Hsinchu 300, Taiwan
[b] Department of Mechanical Engineering, National Chiao Tung University, EE474, 1001 University Road, Hsinchu 300, Taiwan
[c] Department of Engineering and System Science, National TsingHua University, Hsinchu 300, Taiwan

ARTICLE INFO

Article history:
Received 8 December 2011
Received in revised form
5 June 2012
Accepted 18 June 2012
Available online 4 July 2012

Keywords:
Carbon dioxide
Gas cooler
Heat exchanger
Supercritical
Pseudo-critical

ABSTRACT

In this study, a tube-in-tube heat exchanger model applicable to supercritical CO_2 and water was developed. The developed model is first validated with some existing measurements. Normally, the variation of the heat transfer rate for a constant-property working fluid shows a monotonic decrease from the inlet of minimum heat capacity flow rate (C_{min}). By contrast, the CO_2 may present a local minimum and a local maximum along the length of the heat exchanger, provided CO_2 passes through the pseudo-critical temperature, and this phenomenon becomes more and more pronounced when the pressure is close to the critical pressure. In contrast, it is possible for a local maximum heat transfer rate to occur near the inlet of C_{min} even when the CO_2 does not pass through the pseudo-critical point. This happens when C_{min} is on the water side and the property variation of CO_2 is taken into account. The calculation also shows that the effect of the inlet pressure on the variation of the CO_2 temperature is not as apparent as the effect of the inlet pressure on the heat transfer rate, even when there is a significant change in the overall heat transfer coefficient, implying that the heat transfer characteristics of CO_2 near the pseudo-critical region is similar to normal refrigerants, which show an invariant temperature at the condensation point. Hence, it would be beneficial to extend the influence of the pseudo-critical region when taking the heat transfer augmentation into consideration.

Performance d'un refroidisseur de gaz au CO2 à double tube

Mots clés : dioxyde de carbone ; refroidisseur de gaz ; échangeur de chaleur ; supercritique ; pseudo-critique

1. Introduction

The use of natural refrigerants for heating, ventilation, air-conditioning, and refrigeration applications has attracted much attention recently. Among the possible candidates, carbon dioxide (CO_2) is regarded as one of the most promising candidates because it is environmentally benign, nontoxic, and possesses comparatively good thermodynamic properties. Carbon dioxide is also comparable to HCFC refrigerants and outperforms conventional refrigerants when it is used in hot water heaters and automobile air conditioners (Lorentzen and Pettersen, 1993; Lorentzen, 1994; Lorentzen, 1995). In CO_2

* *Corresponding author*. Tel.: +886 3 5712121x55105; fax: +886 3 5720634.
E-mail address: ccwang@mail.nctu.edu.tw (C.-C. Wang).
0140-7007/$ – see front matter
http://dx.doi.org/10.1016/j.ijrefrig.2012.06.010

Nomenclature

A	surface area (m^2)
C	heat capacity flow rate ($W\ K^{-1}$)
Cp	specific heat ($J\ kg^{-1}\ K^{-1}$)
d	diameter (m)
f	friction factor
h	heat transfer coefficient ($W\ m^{-2}\ K^{-1}$)
i	specific enthalpy ($kJ\ kg^{-1}$)
ID	inner diameter (m)
k	conductivity ($W\ m^{-1}\ K^{-1}$)
L	tube length (m)
LMTD	log mean temperature difference (K)
$\dot{m}$	mass flow rate ($kg\ s^{-1}$)
Mw	mass flow rate for water ($kg\ s^{-1}$)
Mc	mass flow rate for CO_2 ($kg\ s^{-1}$)
Nu	Nusselt number ($hd\ k^{-1}$)
OD	outer diameter (m)
P	pressure (MPa)
Pr	Prandtl number
Q	heat transfer rate (kW)
R	thermal resistance ($C\ W^{-1}$)
Re	Reynolds number ($\rho ud\ \mu^{-1}$)
T	temperature (°C)
u	velocity ($m\ s^{-1}$)
U	overall heat transfer coefficient ($W\ m^{-2}\ K^{-1}$)

Greek letters

ΔT	temperature difference (K)
μ	viscosity ($kg\ m^{-1}\ s^{-1}$)
ρ	density ($kg\ m^{-3}$)

Subscripts

b	bulk
c	carbon dioxide
c,i	ith segment of carbon dioxide
f	film
H	hydraulic diameter
i	inner
i	ith segment of the heat exchanger
max	larger one
min	smaller one
o	outer
w	water
wall	wall
w,i	ith segment of the water side

air-conditioning and heat pump systems, CO_2 rejects heat at a pressure above the critical pressure (7.38 MPa) in the gas cooler without phase change. When the CO_2 is at supercritical pressures, some small fluid temperature and pressure variations may produce large changes in the thermophysical properties, and this is especially pronounced when the temperature is near the critical point. The gigantic change in the thermophysical properties may result in significant deviations in both heat transfer and fluid flow behaviors.

In contrast, investigations associated with CO_2 are mainly performed on either system performance (e.g., Austin and Sumathy, 2011; Goodman et al., 2011; Cecchinato et al., 2005) or the heat transfer characteristics between tubes and channels (e.g., Cheng et al., 2008; Dang and Hihara, 2004a, 2004b; Dang et al., 2007, 2008, 2010; Gao et al., 2007; Kim et al., 2008; Liao and Zhao, 2002; Yun et al., 2005, 2007). There are comparatively fewer studies concerning the overall performance of heat exchangers (gas coolers). The relevant studies on the performance of gas coolers are normally classified into two categories—air cooled and water cooled—and most studies were related to air-cooled systems (Asinaria et al., 2004; Chang and Kim, 2007; Park and Hrnjak, 2007; Zhao and Ohadi, 2004; Zilio et al., 2007). Note that the dominant thermal resistances for an air-cooled gas cooler mainly occur on the air side, and thus its performance is normally controlled by the air flow rather than the CO_2, irrespective of appreciable changes in the physical properties of CO_2. In contrast, comparatively fewer studies investigate the water-cooled gas cooler. The only studies investigating the water-cooled gas cooler were carried out by Fronk and Garimella (2011a, 2011b) and Wang and Hihara (2002). The former conducted an analysis of the heat transfer mechanisms of a water-coupled gas cooler with a compact, multipass cross-counter flow of aluminum-brazed plate and a microchannel CO_2 gas cooler and validated the analysis with experimental data. The later presented an analysis of a concentric counterflow heat exchanger by solving a set of complicated partial differential equations, including conservation of mass, momentum and energy equations, between CO_2 and water and considering the wall conduction in both the radial and axial directions. They found that the variation of the local heat flux revealed a local maximum within the heat exchanger due to the tremendous change in the specific heat of CO_2.

For a typical gas cooler, irrespective of the inlet pressure, the temperature of CO_2 changes quite significantly along the length of the heat exchanger and may pass through the pseudo-critical point, where an appreciable change in the heat capacity may occur. In addition, the effect of changes in the physical properties of CO_2 is even more severe for a liquid-cooled gas cooler because the controlled thermal resistance could switch to the CO_2 side. Despite the considerable efforts that were devoted in determining the heat transfer performance of CO_2 above the critical point, the existing studies of liquid-cooled gas coolers are limited and complicated. Hence, it is the objective of this study to develop a simple heat exchanger model that is capable of investigating and analyzing the heat transfer behavior of a CO_2 tube-in-tube water-cooled gas cooler subject to a given set of inlet conditions.

2. Numerical method

The model heat exchanger is a double-pipe heat exchanger with water flowing in the annulus and CO_2 flowing countercurrently in the tube. Fig. 1 is a schematic of the heat exchanger. Because considerable changes in the physical properties of CO_2 may be encountered, especially near pseudo-critical temperatures, the heat exchanger must be subdivided into many small segments. A prior sensitivity analysis of the influence of the segments was performed, and

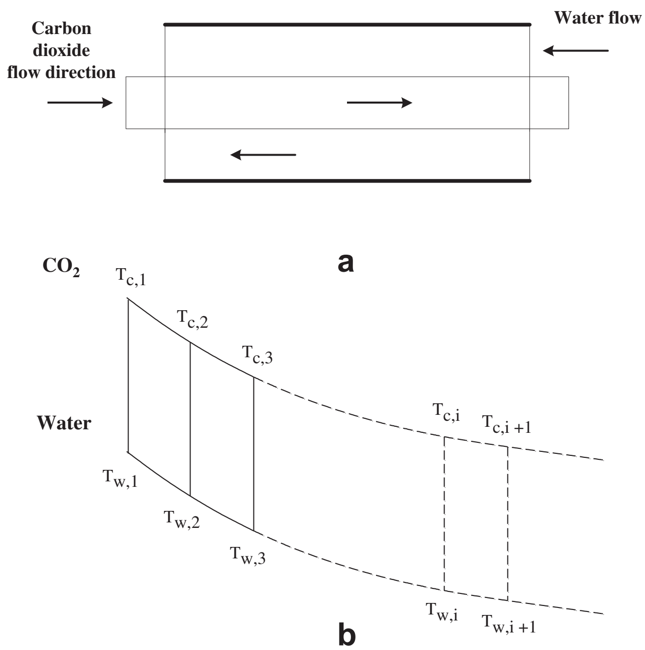

Fig. 1 – (a) Schematic of the tube-in-tube heat exchanger and (b) Definition of the temperature for CO_2 and water along the length of the tube-in-tube heat exchanger.

a total of 65 segments were used in the simulation. A schematic showing the variation of the temperature for CO_2 and water is shown in Fig. 1(b), where the subscript c denotes CO_2 and w represents water. The heat balance between the water and the coolant in each segment i can be expressed by the following equations:

$$Q_i = m_c Cp_{c,i}\left(T_{c,i} - T_{c,i+1}\right) = m_w Cp_{w,i}\left(T_{w,i} - T_{w,i+1}\right). \quad (1)$$

$$Q_i = (UA)_i \times (\mathrm{LMTD})_i. \quad (2)$$

The overall heat transfer coefficient is obtained from

$$\frac{1}{UA} = \frac{1}{h_w A_{o,i}} + \frac{\ln\dfrac{d_o}{d_i}}{2\pi k_{wall} L} + \frac{1}{h_c A_{i,i}}. \quad (3)$$

The physical properties of CO_2 are a function of the local pressure and temperature, and the properties of water are related to the local temperature. The relevant properties are obtained from REFPROP, 2007. The heat transfer coefficient of CO_2 is based on the Dang and Hihara, 2004a, i.e.,

$$h_c = Nu_c k_c / d. \quad (4)$$

$$Nu_c = \frac{\left(\dfrac{f_c}{8}\right)(Re_b - 1000)Pr}{1.07 + 12.7\sqrt{\dfrac{f_c}{8}}\left(Pr^{2/3} - 1\right)}. \quad (5)$$

where

$$Pr = \begin{cases} Cp_b \mu_b / \lambda_b, & \text{for} \quad Cp_b \geq \overline{Cp} \\ \overline{Cp}_b \mu_b / \lambda_f, & \text{for} \quad Cp_b < \overline{Cp} \quad \text{and} \quad \mu_b/\lambda_b \geq \mu_f/\lambda_f \\ \overline{Cp}_b \mu_f / \lambda_f, & \text{for} \quad Cp_b < \overline{Cp} \quad \text{and} \quad \mu_b/\lambda_b < \mu_f/\lambda_f \end{cases}. \quad (6)$$

$$\overline{Cp} = \frac{h_b - h_{wall}}{T_b - T_{wall}}. \quad (7)$$

$$Re_b = \frac{G d_i}{\mu_b}. \quad (8)$$

$$f_c = [1.82 \log(Re_b) - 1.64]^{-2}. \quad (9)$$

where the subscript b represents the bulk temperature, wall is evaluated at the wall temperature and f denotes a calculation at the film temperature. The film temperature, T_f, is defined as $T_f = (T_b + T_{wall})/2$. In contrast, the heat transfer coefficient for the water side, h_w, is obtained via the Gnielinsk (1976) correlation:

$$h_w = Nu_w k_w / d_H. \quad (10)$$

$$Nu_w = \frac{\left(\dfrac{f_w}{8}\right)(Re - 1000)Pr}{1.07 + 12.7\sqrt{\dfrac{f_w}{8}}\left(Pr^{2/3} - 1\right)}. \quad (11)$$

where

$$f_w = [1.82 \log(Re_w) - 1.64]^{-2}. \quad (12)$$

3. Results and discussion

To validate the proposed model, the calculation is first compared with the measurements of Pitla et al. (2000). Pitla et al. (2000) conducted experiments exploiting a CO_2 tube-in-tube heat exchanger with an ID of 0.00472 m and an OD of 0.00635 m for the inner tube. The ID for the outer tube is 0.01575 m. Their test conditions are tabulated in Table 1. Using the inlet conditions for their raw data, the calculated cooling capacity vs. their measurements is depicted in Fig. 2. As seen, the calculations are in line with the experimental measurements, suggesting the applicability of the present modeling.

Fig. 3 is a schematic showing the relevant influence of the local heat transfer rate as a function of position, starting at the inlet of the fluid where the minimum thermal capacitance rate (C_{min}) occurs. Fig. 3(a) depicts a schematic showing the local heat transfer rate vs. the dimensionless distance from the inlet of C_{min} for a typical tube-in-tube heat exchanger using a conventional, subcritical, single-phase fluid such as water/water. In general, the variation in the local heat transfer rate shows only monotonic variation, and the heat transfer rate peaks at the inlet of C_{min}, regardless of whether C_{min} is on

Table 1 – Test conditions for Pitla et al. (2000).

Variant	$T_{CO_2,in}$ (°C)	$P_{CO_2,in}$ (MPa)	$T_{water,in}$ (°C)	Mc (kg s^{-1})	Mw (kg s^{-1})
Run1	121.2	9.44	20.8	0.01963	0.04011
Run2	126	11.19	24.2	0.0274	0.040497
Run3	73.3	13.33	36.12	0.02043	0.12914
Run4	123.5	10.8	27.21	0.02862	0.084087
Run5	107.2	8.11	24.2	0.0198	0.0455
Run6	123.4	8.98	22.3	0.02996	0.067864
Run7	118.3	7.79	21.2	0.02123	0.066434
Run8	115.8	8.60	18.9	0.03436	0.084087
Run9	114.9	8.76	18.9	0.03638	0.065091
Run10	113.4	9.50	15.9	0.03825	0.109052

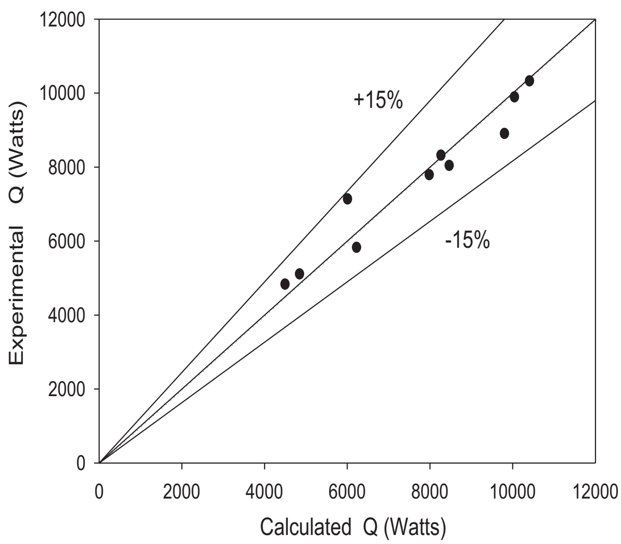

Fig. 2 – Comparison of the local heat transfer rate for the calculations and Pitla et al.'s data (2000).

the hot side or the cold side, followed by a steady decrease from the inlet of C_{min} toward the outlet. In an extreme case in which $C_{min} = C_{max}$, the variation of the local heat transfer rate remains unchanged, provided the overall heat transfer coefficient is unchanged, as shown in Fig. 3(b).

Apart from the constant-property condition, appreciable changes in the thermophysical properties of CO_2 give rise to some certain unique characteristics. Of course, the variation in the local heat transfer rate for a CO_2 heat exchanger still behaves quite similarly to the constant-property scenario (Fig. 3(a)) as long as the CO_2 does not pass the pseudo-critical point. Aside from the conventional monotonic behavior, there are two special phenomena that may be seen for the CO_2 heat exchanger, namely, a local minimum and a plateau (Fig. 3(c)) and a local maximum may occur within the heat exchanger (Fig. 3(d)). To illustrate these special phenomena, calculations are performed with a CO_2 tube-in-tube heat exchanger with an ID = 0.020 m and an OD = 0.025 m for the inner tube and an ID = 0.050 m for the outer tube. The calculations are made for inlet pressures of 12, 10, and 8 MPa. The inlet temperatures of CO_2 and water are 382 K and 287 K, respectively, while the mass flow rates for water and CO_2 are both 0.5 kg s^{-1}. The variation of the local heat transfer rate as a function of the dimensionless tube length is shown in Fig. 4(a). As clearly seen in this figure, the CO_2 heat exchanger shows a peculiar trend compared with that of constant-property fluids. The local heat transfer rate does not show a consistently monotonic decrease from the inlet of C_{min} along the length of the heat exchanger. Conversely, the local heat transfer rate first decreases to a local minimum, followed by a rise to a plateau, and finally decreases again toward the outlet. This strange phenomenon becomes more and more apparent when the inlet pressure is further reduced. In fact, a significant recovery of the local heat transfer rate is encountered for $p = 8$ MPa, despite the fact that the maximum temperature difference still occurs at the CO_2 inlet. To explain this phenomenon, one must understand the variation of the specific heat capacity of CO_2 above the critical point, as shown in Fig. 4(b). For a given supercritical pressure, a sharp rise in the c_p is seen at the so-called pseudo-critical temperature. In practice, when cooling, the very hot CO_2 gas may inevitably pass through this temperature. In this sense, a significant increase in c_p is seen near this temperature, leading to an increase in the heat transfer coefficient and a much larger overall heat transfer coefficient accordingly. This phenomenon becomes even more pronounced when the pressure is further decreased as c_p increases near the critical point. As a result, a significant recovery of the local heat transfer rate and a second maximum occur in the tube-in-tube heat exchanger. The temperature variation of CO_2 as a function of the tube length is depicted in Fig. 4(c). The effect of the inlet pressure on the variation of the CO_2 temperature is not as apparent as the variation of the heat transfer rate, even when there is a significant change in the overall heat transfer coefficient. One of the explanations involves the considerable increase in the heat capacity flow rate (C) of the CO_2 near the pseudo-critical temperature. Based on a simple energy balance formula, $Q = C_c \Delta T$, it is not surprising that the variation of the CO_2 temperature tends to show a very slowly decreasing trend adjacent to the pseudo-critical region when compared with the inlet or outlet region. Apparently, this phenomenon becomes more pronounced as the inlet pressure is decreased, thereby leading to intersections of the temperatures profiles along the length of the heat exchangers. The foregoing results imply that the heat transfer characteristics of CO_2 near the pseudo-critical region resemble normal refrigerants, which show an invariant temperature at the condensation point.

In contrast, it is possible for a local maximum to occur near the inlet of C_{min} (Fig. 3(d)) even when CO_2 does not pass through the pseudo-critical point. This occurs when C_{min} is on the water side and the effect of the variable properties has

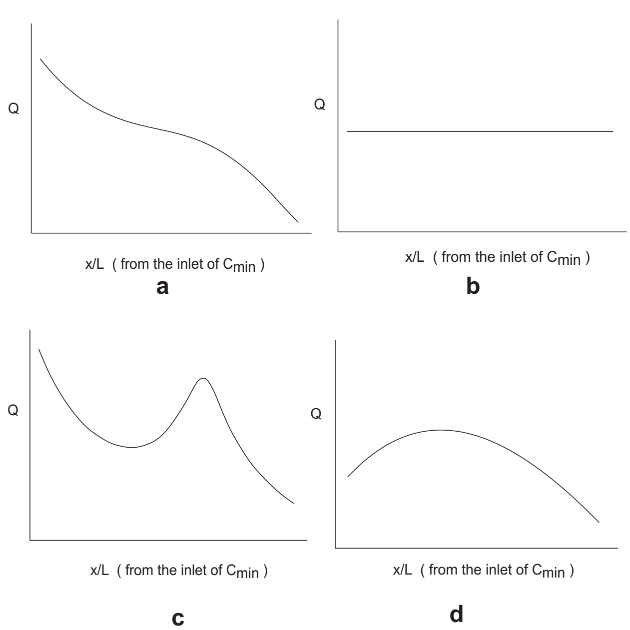

Fig. 3 – Schematic of the variation of the local heat transfer rate for a tube-in-tube heat exchanger: (a) Constant property, $C_{min} \neq C_{max}$; (b) Constant property, $C_{min} = C_{max}$; (c) CO_2 flow across the pseudo-critical point; and (d) Variable property.

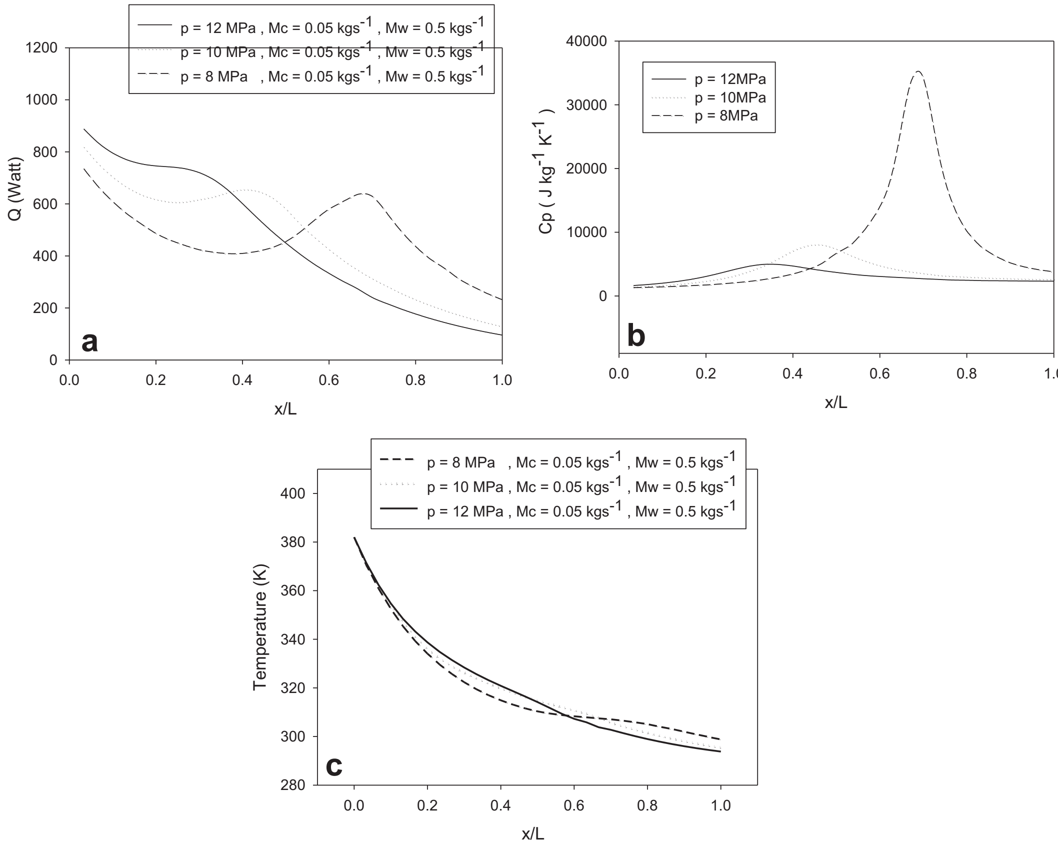

Fig. 4 – Effect of the inlet pressure on (a) The variation of the local heat transfer rate vs. the dimensionless tube length, (b) The variation of c_p vs. the dimensionless tube length and (c) The variation of the CO_2 temperature vs. the dimensionless tube length.

been accounted for. Basically, the recovery of the local heat transfer rate is quite small and could also be applicable to any working-fluid subject to the same conditions.

4. Concluding remarks

The present study described a tube-in-tube heat exchanger model applicable for supercritical CO_2 and water. The developed model is validated with some existing measurements. In addition, a further calculation is made to examine the influence of the inlet pressure of CO_2 on the heat transfer performance. Normally, the variation of the local heat transfer rate for constant-property working fluids shows a monotonic decrease from the inlet of C_{min}. Conversely the CO_2 may present a local minimum and a local maximum along the length of the heat exchanger, provided CO_2 passes through the pseudo-critical temperature, and this phenomenon becomes more and more pronounced when the pressure is close to the critical pressure. The phenomenon is attributed to the significant increase in the specific heat of CO_2 near the pseudo-critical temperature. The calculation also shows that the effect of the inlet pressure on the variation of the CO_2 temperature is not as apparent as the variation of the heat transfer rate, even when there is a significant change in the overall heat transfer coefficient. This is also associated with a considerable increase in the heat capacity flow rate of the CO_2 near the pseudo-critical temperature. As a consequence, the variation of the CO_2 temperature tends to show a very slow decreasing trend adjacent to the pseudo-critical region when compared with the inlet or outlet region. Apparently, this phenomenon becomes more pronounced as the inlet pressure is decreased, thereby leading to intersections of the temperatures profiles along the length of the heat exchangers. The foregoing results imply that the heat transfer characteristics of CO_2 near the pseudo-critical region resemble those of normal refrigerants, which show an invariant temperature at the condensation point. Hence, it would be beneficial to expand the influence of the pseudo-critical region when considering heat transfer augmentation.

In contrast, it is possible for a local maximum heat transfer rate to occur near the inlet of C_{min}, even when CO_2 does not pass through the pseudo-critical point. This happens when C_{min} is on the water side and the variation in the CO_2 properties is taken into account.

Acknowledgments

The authors would like to express gratitude for the Energy R&D foundation funding from the Bureau of Energy of the Ministry of Economic, Taiwan, and the National Science Committee (NSC 100-ET-E-009-004-ET) of Taiwan.

REFERENCES

Asinaria, P., Cecchinato, L., Fornasieri, E., 2004. Effects of thermal conduction in microchannel gas coolers for carbon dioxide. Int. J. Refrigeration 27, 577–586.

Austin, B.T., Sumathy, K., 2011. Parametric study on the performance of a direct-expansion geothermal heat pump using carbon dioxide. Appl. Thermal Eng. 31, 3774–3782.

Cecchinato, L., Corradi, M., Fornasieri, E., Zamboni, L., 2005. Carbon dioxide as refrigerant for tap water heat pumps: a comparison with the traditional solution. Int. J. Refrigeration 25, 1250–1258.

Cheng, L., Ribatski, G., Thome, J.R., 2008. Analysis of supercritical CO_2 cooling in macro- and micro-channels. Int. J. Refrigeration 31, 1301–1316.

Chang, Y.S., Kim, M.S., 2007. Modeling and performance simulation of a gas cooler for a CO_2 heat pump system. HVAC&R Res. 13, 445–456.

Dang, C., Hihara, E., 2004a. In-tube cooling heat transfer of supercritical carbon dioxide part 1: experimental measurement. Int. J. Refrigeration 24, 736–747.

Dang, C., Hihara, E., 2004b. In-tube cooling heat transfer of supercritical carbon dioxide part 2: comparison of numerical calculation with different turbulence models. Int. J. Refrigeration 24, 748–760.

Dang, C., Iino, K., Fukuoka, K., Hihara, E., 2007. Effect of lubricating oil on cooling heat transfer of supercritical carbon dioxide. Int. J. Refrigeration 30, 724–731.

Dang, C., Iino, K., Hihar, E., 2008. Study on two-phase flow pattern of supercritical carbon dioxide with entrained PAG type lubricating oil in a gas cooler. Int. J. Refrigeration 31, 1265–1272.

Dang, C., Iino, K., Hihara, K., 2010. Effect of PAG-type lubricating oil on heat transfer characteristics of supercritical carbon dioxide cooled inside a small internally grooved tube. Int. J. Refrigeration 33, 558–565.

Fronk, B.M., Garimella, S., 2011a. Water-coupled carbon dioxide microchannel gas cooler for heat pump water heaters: part I – experiments. Int. J. Refrigeration 34, 7–16.

Fronk, B.M., Garimella, S., 2011b. Water-coupled carbon dioxide microchannel gas cooler for heat pump water heaters: part II – model development and validation. Int. J. Refrigeration 34, 17–28.

Gao, L., Honda, T., Koyama, S., 2007. Experiments on flow boiling heat transfer of almost pure CO_2 and CO_2–oil mixtures in horizontal smooth and microfin tubes. HVAC&R Res. 13, 415–425.

Gnielinsk, V., 1976. New equation for heat and mass transfer in turbulent pipe and channel flow. Int. Chem. Eng. 16, 359–368.

Goodman, C., Fronk, B., Garimella, S., 2011. Transcritical carbon dioxide microchannel heat pump waterheaters: part II – system simulation and optimization. Int. J. Refrigeration 34, 870–880.

Kim, H., Hwan, Y.K., Song, J.H., 2008. Heat transfer to supercritical pressure carbon dioxide flowing upward through tubes and a narrow annulus passage. Prog. Nucl. Energy 50, 518–525.

Liao, S.M., Zhao, T.S., 2002. An experimental investigation of convection heat transfer to supercritical carbon dioxide in miniature tubes. Int. J. Heat Mass Trans. 45, 5025–5034.

Lorentzen, G., Pettersen, G., 1993. A new efficient and environmentally benign system for car air-conditioning. Int. J. Refrigeration 16, 4–12.

Lorentzen, G., 1994. Revival of carbon dioxide as a refrigerant. Int. J. Refrigeration 17, 292–301.

Lorentzen, G., 1995. The use of natural refrigerants: a complete solution to the CFC/HCFC predicament. Int. J. Refrigeration 18, 190–197.

Park, C.Y., Hrnjak, P., 2007. Effect of heat conduction through the fins of a microchannel serpentine gas cooler of transcritical CO_2 system. Int. J. Refrigeration 30, 389–397.

Pitla, S.S., Robinson, D.M., Zingerli, A., Groll, E.A., Ramadhyani, S., 2000. Heat transfer and pressure drop during in-tube gas cooling of supercritical carbon dioxide, ASHRAE Research Project Report, pp. 3613–3621.

REFPROP, 2007. Thermodynamic Properties of Refrigerants and Refrigerant Mixtures, Version 8.0. National Institute of Standards and Technology, Gaithersburg, MD.

Wang, J.F., Hihara, E., 2002. Study on carbon dioxide gas cooler heat transfer process under supercritical pressures. Int. J. Energy Res. 26, 1237–1251.

Yun, Y., Min, Y., Kim, M.S., 2005. Flow boiling heat transfer of carbon dioxide in horizontal mini-tubes. Int. J. Heat Mass Trans. 26, 801–809.

Yun, R., Hwang, Y., Radermacher, R., 2007. Convective gas cooling heat transfer and pressure drop characteristics of supercritical CO_2/oil mixture in a minichannel tube. Int. J. Heat Mass Trans. 50, 4796–4804.

Zhao, Y., Ohadi, M.M., 2004. Experimental study of supercritical CO_2 gas cooling in a microchannel gas cooler. ASHRAE Trans. 110 (1), 291–300.

Zilio, C., Cecchinato, L., Corradi, M., Schiochet, G., 2007. An assessment of heat transfer through fins in a fin-and-tube gas cooler for transcritical carbon dioxide cycles. HVAC&R Res. 13, 457–469.